Pergamon

PII: S0191-8141(96)00100-9

Journal of Structural Geology, Vol. 19, No. 5, pp. 639 to 652, 1997

0191-8141/97 $17.00 + 0.00

Strain and strain rate in a synkinematic trondhjemitic dike: evidence for melt-induced strain softening during shearing (Bohemian Massif, Czech Republic)

GERNOLD ZULAUF and STEFAN HELFERICH

Geologisch-Paläontologisches Institut, Universität Frankfurt a.M., Senckenberganlage 32–34, D 60054 Frankfurt a.M., Germany

(*Received* 11 *October* 1995; *accepted in revised form* 11 *November* 1996)

Abstract—Emplacement-related deformation of a Cambrian trondhjemitic dike, located at the western border of the Teplá–Barrandian unit (central European Variscides), is studied in detail. The trondhjemitic melt was emplaced at $T = 750°C$ into an active low-temperature (ca 350°C) east-northeast trending dextral transcurrent shear zone. Thermal modelling indicates that the rheologically critical melt fraction and the solidus of the dike were achieved after 1 and 3 days of cooling, respectively. The major part of the shearing occurred within 8 days after the melt emplaced.

The zonation of the dike, in strain magnitude, mineralogy and geochemistry, can be explained by the laterally varying rheology (from margin to centre) during cooling and shearing. The deformation was volume-constant, and the strain data plot in the apparent constrictional field. The unusually high value of the calculated longitudinal strain rate ($> 2.8 \times 10^{-6}$ s^{-1}; equivalent to a displacement rate of > 2 cm h^{-1}) is probably related to the intruding melt that 'lubricated' the shear zone and thus enhanced its displacement velocity. Consequently, melts that intrude as dikes into active transcurrent shear zones may significantly weaken the strength of the middle and upper continental crust. © 1997 Elsevier Science Ltd.

INTRODUCTION

It is widely accepted that granitoid magmas may ascend through the continental crust via brittle fracture zones (Castro, 1987; Guineberteau *et al.*, 1987; Hutton, 1988, 1992; Wolf and Saleeby, 1992; Castro *et al.*, 1995; Karlstrom and Williams, 1995). Several natural examples of fault-controlled magmatism suggest that melts may passively intrude into contractional shear zones (Karlstrom *et al.*, 1993; Ingram and Hutton, 1994; Nyman *et al.*, 1994), strike-slip regimes (Hutton and Reavy, 1992 and references therein), and extensional structures (Hutton *et al.*, 1990; Aranguren and Tubia, 1992; Hudec, 1992; Lister and Baldwin, 1993; Parsons and Thompson, 1993). In cases where melts intrude as dikes or emplace into active normal faults, the common space problem hardly occurs (Hutton *et al.*, 1990; Paterson and Fowler, 1993).

Magmatic dikes are commonly oriented perpendicular to the least principal stress (Suppe, 1985; Emerman and Marrett, 1990). Their emplacement is favored by pre-existing fractures that are filled and widened by the melt. The internal fluid pressure of the magma may considerably reduce the effective stress, thus triggering crack propagation by hydrofracturing even in contractional tectonic settings (Spence and Turcotte, 1985; Sleep, 1988; Clemens and Mawer, 1992; Petford *et al.*, 1993). Where the migrating melt invades active shear zones, the shear strength may significantly decrease leading to a rise in the strain rate. Consequently, the melt-lubricated shear zone will continue to deform more easily than the surrounding rocks (Hollister and Crawford, 1986).

Since at upper crustal levels the crystallization time of a magma is generally short compared with rate of deformation (Paterson and Tobisch, 1988, 1992), we are able to determine the age of the deformation by dating synkinematically emplaced plutons or dikes. Moreover, in certain cases the strain rate can be estimated by considering strain and cooling data of a magmatic body (John and Blundy, 1993; Karlstrom *et al.*, 1993). This particularly holds for magmatic dikes. If dikes emplace within active brittle to brittle–ductile shear zones of the upper crust, the melt will cool down very rapidly.

In the present study we have investigated a trondhjemitic dike and its country rocks located in the Domažlice crystalline complex at the western border of the Teplá–Barrandian unit (central European Variscides). The dike intruded synkinematically into an early Palaeozoic transcurrent shear zone. We determined the temperature of both the dike magma and the country rock. These data were used to carry out a thermal modelling that yields constraints on the thermal history during and after melt emplacement. Using strain data derived from the dike, we calculated the strain rate of the 'hot-dike-shearing' event.

REGIONAL GEOLOGY

The Domažlice crystalline complex is situated in the south-western part of the Teplá–Barrandian unit (see inset in Fig. 1). The latter consists of a Cadomian basement with moderate Variscan tectono-metamorphic imprints (Chlupáč, 1993). The rocks of the Domažlice crystalline complex include metagreywackes, metasiltstones, and minor metabasites all of which show evidence of a Cadomian Barrovian-type metamorphism (Vejnar, 1982; Zulauf *et al.*, 1997).

The grade of the Barrovian-type metamorphism increases considerably from east-northeast (lowermost greenschist facies) to west-southwest (amphibolite

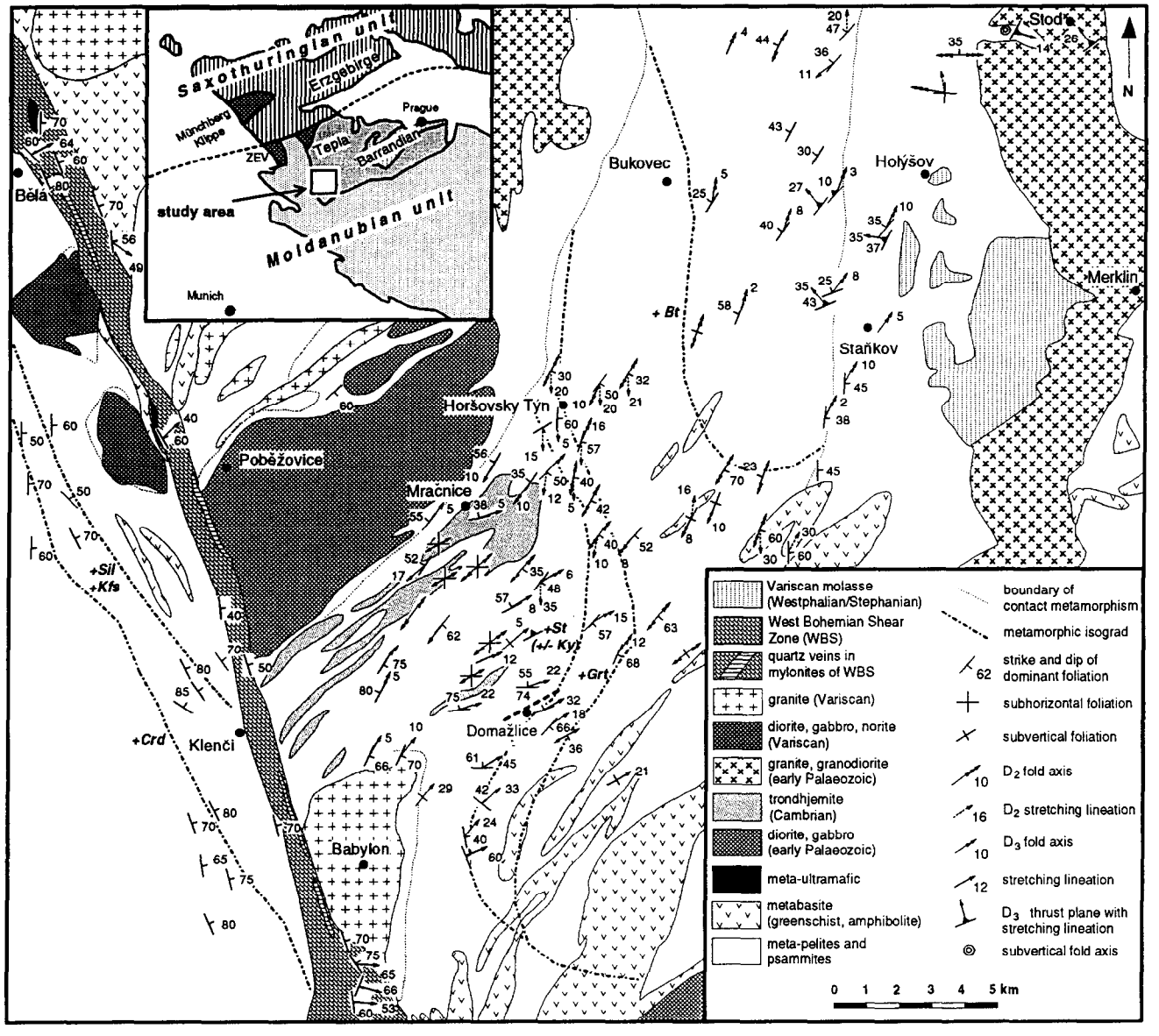

Fig. 1. Geological map of the Domažlice area with structural data; lithology and metamorphic isograds are reproduced from Vejnar (1982, 1984). Isograds: Bt = biotite, Grt = garnet, St (±Ky) = staurolite (including occurrence of rare kyanite), Sil + Kfs = sillmanite + K-feldspar, Crd = cordierite. The trondhjemitic dike studied is marked by a thick dashed line near Domažlice.

facies). This situation is well documented by metamorphic isograds (biotite, garnet, staurolite ± kyanite isograd, Vejnar, 1982) that are cut by the Carboniferous West Bohemian Shear Zone (Zulauf, 1994; see also Fig. 1).

The structural evolution of the Domažlice area is polyphase. It has been described in detail from the eastern greenschist facies part where the Cambrian Stod pluton (Dörr *et al.*, 1995) allows separation of Cadomian and Variscan events. D_1 and D_2 as well as the Barrovian-type metamorphism belong to the Cadomian cycle (Zulauf, 1995). The Variscan convergence (D_3) was associated with retrograde (greenschist facies) metamorphism, east-southeast directed thrusting, and weak folding.

In the western, amphibolite facies part of the Domažlice crystalline complex, additional east-northeast to northeast trending transcurrent and transtensional (oblique-slip normal) shear zones developed between D_2 and D_3. Moreover, there are several types of large plutons that formed extensive zones of contact metamorphism. Conventional U–Pb dating of zircons, separated from the large, northeast trending Mračnice trondhjemite (Fig. 1), yields a well-defined discordia with a lower intercept at 523 + 4/−5 Ma (Dörr *et al.*, 1995; Zulauf *et al.*, 1997). This age is interpreted as the intrusion age. It is compatible with ages derived from pegmatites that cut through the trondhjemites and related trondhjemitic dikes. Rb–Sr dating of large undeformed white mica from these pegmatites yields ages between 485 and

501 Ma (Košler *et al.*, 1994; Glodny *et al.*, 1995). These are interpreted as being close to the time of pegmatite emplacement.

The present study will focus on the northeast to east-northeast trending trondhjemitic dikes that are up to 5 m in width. Their internal structure varies significantly from almost non-foliated (porphyritic) to strongly foliated (mylonitic). We investigated a dike that belongs to the latter type from the quarry 'Hvízdalka' at the north-eastern margin of Domažlice (Fig. 1).

COUNTRY ROCK OF THE TRONDHJEMITIC DIKE

Composition, structure and kinematics

The country rocks of the dike consist of paragneiss and phyllonite. The phyllonites result from pervasive shearing along east-northeast trending transcurrent shear zones that cut the entire quarry under retrograde metamorphic conditions. They display a pronounced lineation consisting of pressure shadows adjacent to garnet, elongated aggregates of quartz and feldspar, mica fishes and chlorite, which plunges 20–30° east-northeast, mostly on steeply north-northwest dipping planes (Fig. 2). Macroscopic shear sense indicators like *S–C* and shear band fabrics clearly indicate a dextral displacement that was also confirmed under the microscope using drag structures in micas as well as asymmetric pressure shadows of chlorite behind rigid porphyroclasts of garnet, sillimanite, muscovite and biotite (Fig. 3a & b).

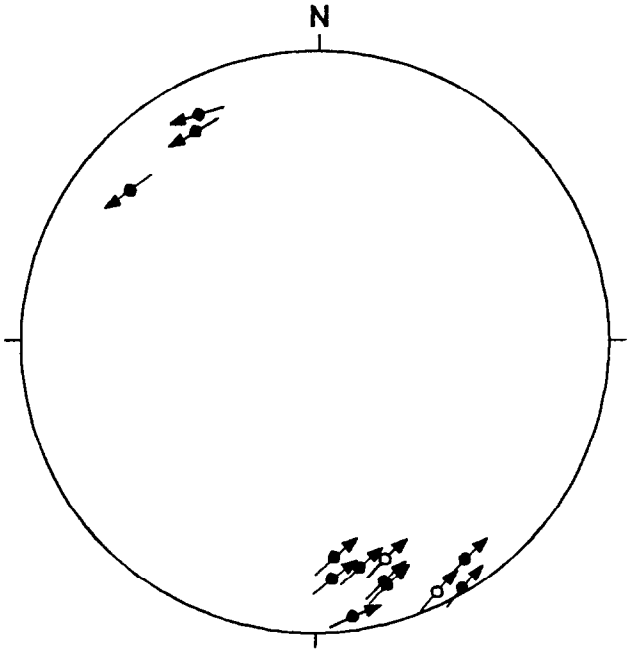

Fig. 2. Structural data in the transcurrent shear zone. The direction of the stretching lineation is represented on the pole of the mylonitic foliation; arrow indicates the transport direction of the hanging wall according to the method of Hoeppener (1955). Full circles indicate the poles to the mylonitic foliation in the country rocks, and open circles the poles to the mylonitic foliation in the trondhjemitic dike. Lower-hemisphere equal-area plot.

SG 19-5-C

Within the sheared phyllonite, the primary minerals of the paragneiss are strongly altered. Garnet is replaced by biotite, and sometimes both minerals are altered to chlorite. Plagioclase, sillimanite and staurolite are sericitized. In high-strain areas garnet and staurolite display pervasive fracturing. Micas are also broken but rather show bending and kinking. Deformation features in quartz include subgrain boundaries aligned parallel to the prism planes, and grain boundary migration associated with local dynamic recrystallization (Fig. 3c). Plagioclase is deformed by fracturing and cataclasis.

Right at the contact with the trondhjemitic dike, retrograde metamorphism is absent in the wall rock, although intensive shearing occurred at this site as well; plagioclase is hardly sericitized, and biotite, muscovite and garnet are preserved, although bending, kinking and fracturing of these minerals are common features. Chlorite is completely lacking. Grain boundary migration structures in quartz are more pronounced than further away from the contact (Fig. 3d).

Quartz c-axis fabrics in transcurrent shear zones

In order to determine temperature-dependent transitions in the operative glide systems in quartz when approaching the trondhjemitic dike, quartz *c*-axis fabrics within the mylonitic shear zones were measured on sections cut perpendicular to the mylonitic foliation and parallel to the stretching lineation, using a Universal stage. Two samples were considered, one close to the dike, at 40 cm from the contact and the other taken from a shear zone approximately 10 m from the dike. Both samples are mylonites belonging to the transcurrent movement zone that include *S* and *C* domains (*sensu* Berthé *et al.*, 1979). Since *S* and *C* domains may display different quartz *c*-axis patterns (Krohe, 1990), *C* domains, which are the principal movement zones in sheared quartz veins, were particularly considered when measuring the quartz fabrics.

Both samples show markedly different quartz *c*-axis patterns (Fig. 4). In the shear zone 10 m away from the dike, the *c*-axes form a significant maximum parallel to the *Z*-axis of the finite strain ellipsoid ('basal' maximum of Bouchez and Pecher, 1981; Fig. 4a & b) Additional submaxima occur at *Y* ('prismatic submaximum') and in an intermediate position ('rhomb' submaximum) in a plane dextrally rotated at 35° around *Y* with respect to the *Y–Z* plane. Combining the 'basal' maximum with the other submaxima, a poorly defined asymmetric crossed girdle, with a small opening angle is defined (Fig. 4a).

In the sample located close to the dike, *c*-axes form a well-defined type II crossed girdle (*sensu* Lister and Williams, 1979) with 'prismatic', 'rhomb', and 'basal' submaxima (Fig. 4c & d). In the latter diagram, the

opening angle of the girdles is larger, the 'basal' maxima are weaker and the 'prismatic' and 'rhomb' maxima are stronger than in Fig. 4(a).

Although the 'skeletal outline' (*sensu* Lister and Williams, 1979) of the girdles is difficult to define, a dextral sense of shear can be derived from the girdle asymmetry with respect to the *C* and *S* planes. This is compatible with the dextral sense of shear described previously. The diagrams also help to constrain the operative glide systems in quartz, which seems to have been dominantly on $<a>$; basal slip predominated in the sample 10 m away from the dike, whereas glide on the prism and rhombohedral planes prevailed in the sample located close to the dike.

Geothermometry and metamorphic record

The sequence of mineral parageneses observed in the area reflects a pressure–temperature path related to the Cadomian orogeny. It starts with crustal thickening, indicated by the Barrovian-type mineral assemblages, followed by relatively low-pressure metamorphism (growth of sillimanite) attributed to fast exhumation and/or magmatic activity (Zulauf *et al.*, 1997). Obviously, final uplift was associated with transcurrent and transtensional retrograde movement along the east-northeast to northeast trending shear zones described above. These movements began in the stability field of biotite as is indicated by biotite pressure shadows on garnet. Subsequent growth of chlorite and sericite, together with the deformation and incipient recrystallization of quartz, suggest that the shearing ceased under lower greenschist facies conditions.

Since temperature during shearing is an important variable for thermal modelling as presented below, the chlorite geothermometer was applied to our material. Table 1 gives the compositions of chlorites, formed in pressure shadows of garnet and as pseudomorphs after biotite. It was determined with a CAMEBAX electron microprobe (University of Mainz) with natural wollastonite (Si, Ca), feldspars (Al, Na, K), and synthetic oxides (Ti, Fe, Mg) as standards. We applied the chlorite geothermometers of Cathelineau and Nieva (1985), Cathelineau (1988), and Jowett (1991), all of which are based on the strong temperature dependence of Al(IV) in chlorite. Prerequisites for correct use of the Al(IV) method are relatively low pressures and Al-saturated conditions during chlorite growth. As the dike emplaced at a supracrustal level (see below), where the Al-rich phase sillimanite was replaced by white mica, these conditions can be assumed to apply in our case. The geothermometer yields temperatures around 350°C compatible with the lower greenschist facies conditions derived by the syn-kinematic mineral paragenesis. This is consistent with the observed predominance of basal $<a>$ glide in quartz in the shear zone located 10 m away from the dike (Tullis *et al.*, 1973; Bouchez and Pecher, 1981; Krohe, 1990; Hippertt, 1994 and references therein).

The intrusion depth of the dike is assumed to be 7 km, i.e. similar to that of the nearby Pobežovice and Mračnice plutons (Zulauf *et al.*, 1997), yielding a geothermal gradient of about 50°C km^{-1}. This considerably elevated gradient can be explained as follows: (1) the Cadomian regional metamorphism ceased in the stability field of sillimanite indicating relatively low pressures; (2) the emplacement of the trondhjemitic dikes of the Domažlice crystalline complex clearly post-dates the intrusion of the nearby mafic to intermediate plutons. According to thermal modelling data (Zulauf *et al.*, 1996) these plutons heated the country rocks significantly to temperatures in access of 500°C. This also holds for the area of Domažlice where the trondhjemitic dike is located.

TRONDHJEMITIC DIKE

Composition, structure, kinematics and age

Two trondhjemitic dikes, 50 m apart and about 1 m in width, follow the steep, east-northeast trending transcurrent shear zones of the quarry 'Hvízdalka'. Both dikes are strongly foliated and show a pronounced chilled margin, up to 0.8 cm in width (Fig. 3f & g). The dike foliation, more intense than the shear-zone foliation of the country rock, is present everywhere in the dike including its chilled margin. The foliation plane displays a conspicuous stretching lineation defined by strongly stretched plagioclase and quartz (Fig. 3f). The foliation plane and stretching lineation in the dike are strictly concordant with the structures of the shear zones in the country rocks (Fig. 2). The dextral shear sense, derived from *S–C* fabrics in the dikes (Fig. 3g), is also compatible with that of the wall rock. Detailed investigations, including

Fig. 3. Shear zone fabrics in the country rock (a–d) and trondhjemitic dike (e–g). (a) Photomicrograph of asymmetric pressure shadows of white mica and chlorite on a pseudomorph of vermiculite, sericite and chlorite after garnet showing a dextral sense of shear. The matrix contains quartz, plagioclase, white mica and chlorite; plane polarized light. (b) Photomicrograph of shear band fabric within a retrograde paragneiss layer indicating a dextral sense of shear; the bright layers displaced by the shear bands in the lower part of the photograph are quartz veins. Plane polarized light. (c) Subgrains, strain-induced grain boundary migration and incipient recrystallization structures in quartz of a shear zone located about 10 m away from the dike; crossed polarizers. (d) Subgrains and migration recrystallization structures in quartz at about 40 cm away from the dike; crossed polarizers. (e) Photomicrograph of the dike/wall rock contact; the wall rock (left) consists of quartz, plagioclase, biotite and white mica; the margin of the dike includes recrystallized phenocrysts of plagioclase, quartz and biotite; plane polarized light. (f) Photograph of the sheared trondhjemitic dike showing the principal planes of the finite strain ellipsoid; scale bar = 1 cm. (g) *X–Z*-section of the sheared dike and its wall rock (dark zone at the left-hand side of the photo); note the fine-grained chilled margin and the *S–C* fabric that clearly indicates a sinistral sense of shear (dextral in the field); scale bar = 1 cm.

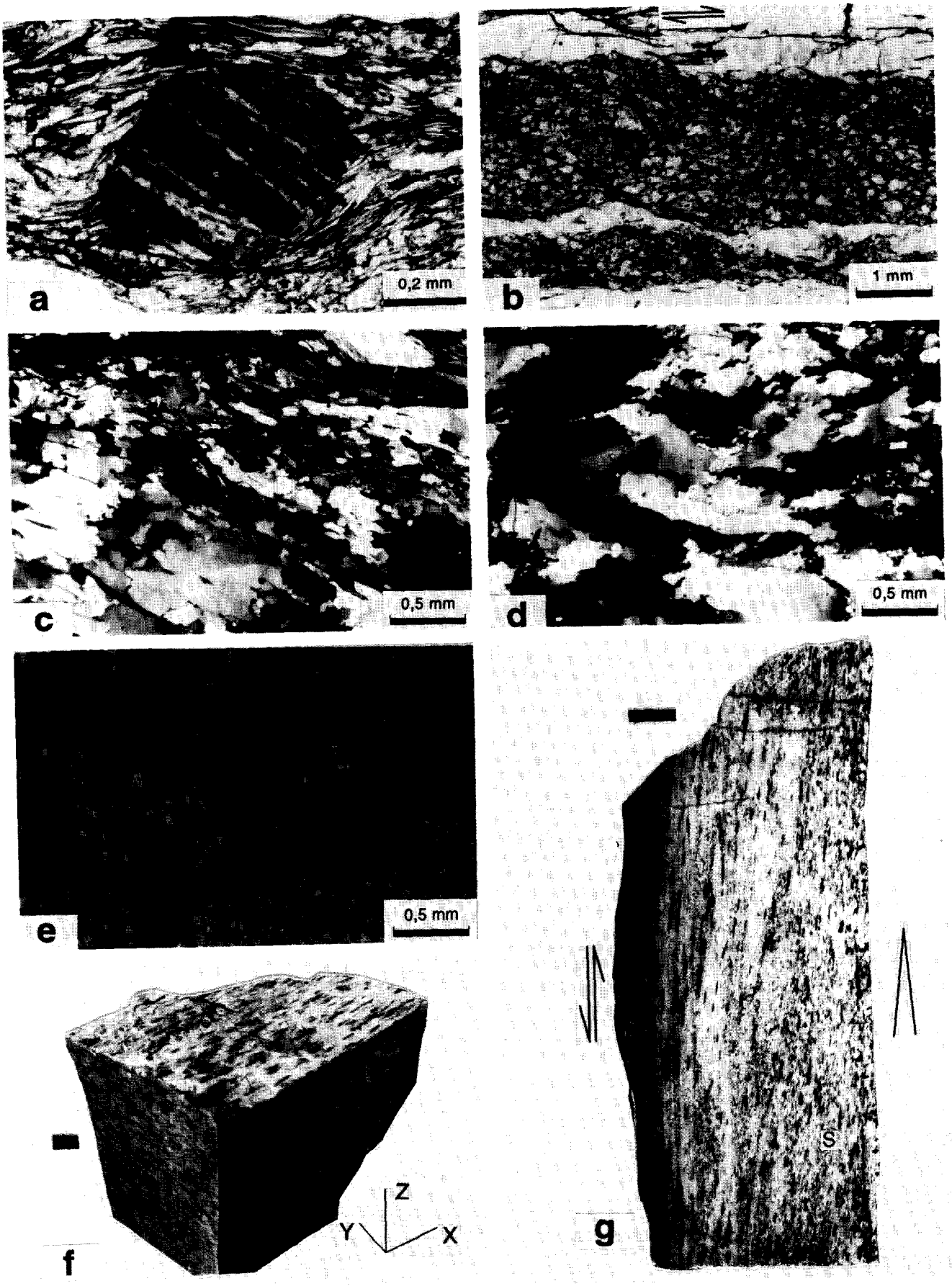
a
0,2 mm
b
1 mm
c
0,5 mm
d
0,5 mm
e
0,5 mm
f
Z
Y
X
g
S

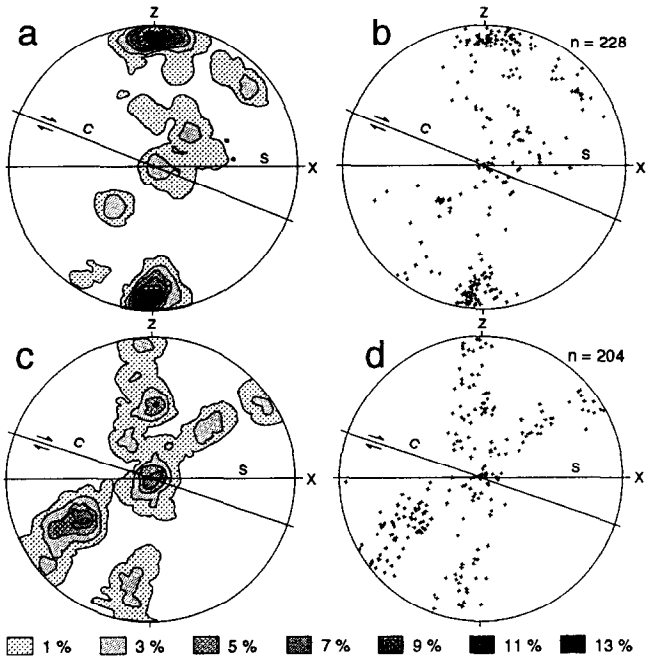

Fig. 4. Quartz *c*-axes distribution in *X*–*Z* sections of the country-rock transcurrent shear zone (lower-hemisphere equal-area plot). (a) and (b) at ca 10 m from the dike. (c) and (d) at ca 40 cm from the dike (see text).

conventional and cathodoluminescence microscopy, XRD, XRF and microprobe analyses, strain measurements, and thermal modelling, have been carried out on the northern dike.

Microscopic investigations as well as XRD and XRF analyses show that the central part of the dike is strikingly different from the chilled margin. The latter consists primarily of quartz (25%), plagioclase (72%), and biotite (2%), while the central part of the dike is rich in quartz (32%) and white mica (20%) and lower in plagioclase (48%). The composition of plagioclase depends on its degree of recrystallization: primary non-recrystallized magmatic crystals have a higher anorthite and K-feldspar component (An_{20-22}, $Or_{1.1-1.6}$) than the recrystallized grains (An_{12-18}, $Or_{0.3-0.6}$) (Fig. 5). Biotite and K-feldspar are very rare in the dike.

The conspicuous mineralogical variation between the centre and margin of the dike is compatible with the geochemistry determined by XRF chemical analyses (Fig. 6). The amount of K_2O, Rb, and Sr drop drastically towards the chilled margin, whereas the amount of Na_2O increases.

The age of the dike should be close to that of the nearby Mračnice trondhjemite (523 Ma, see above). This is supported by the following facts: (1) the mineralogy and geochemistry of the Mračnice body and the trondhjemitic

Table 1. Chemical composition (microprobe analyses) of dike plagioclase and wall-rock chlorite (porph. = plagioclase porphyroclast; matrix = recrystallized plagioclase)

	Plagioclase in dike									Chlorite in wall rock		
	1 porph.	5 porph.	10 matrix	114 matrix	116 matrix	120 matrix	123 matrix	126 matrix		10	12	13
SiO_2	62.99	62.72	64.38	65.45	65.12	64.77	64.52	65.74	SiO_2	24.33	24.61	24.98
Al_2O_3	23.18	23.05	22.42	21.76	21.96	22.17	22.19	21.41	Al_2O_3	19.83	21.10	20.54
FeO	0.07	0.00	0.04	0.01	0.00	0.00	0.12	0.00	FeO	26.24	25.33	26.36
MnO	0.00	0.05	0.02	0.00	0.03	0.03	0.02	0.04	MnO	0.31	0.24	0.37
Na_2O	8.51	8.85	8.91	9.70	9.60	9.35	9.37	9.93	Na_2O	0.00	0.00	0.00
K_2O	0.28	0.19	0.08	0.07	0.07	0.09	0.10	0.05	K_2O	0.02	0.03	0.00
MgO	0.00	0.00	0.00	0.00	0.02	0.00	0.01	0.00	MgO	12.65	13.98	12.44
CaO	4.41	4.12	3.53	2.98	2.94	3.22	3.78	2.49	CaO	0.15	0.06	0.08
TiO_2	0.00	0.00	0.02	0.03	0.02	0.00	0.02	0.00	TiO_2	0.02	0.07	0.00
Cr_2O_3	0.01	0.01	0.01	0.00	0.05	0.00	0.02	0.00				
									Total	83.55	85.43	84.77
Total	99.45	98.99	99.40	99.99	99.81	99.62	100.16	99.65				
									Si	5.45	5.34	5.50
Si	2.80	2.80	2.85	2.88	2.87	2.86	2.84	2.89	Al(IV)	2.55	2.66	2.50
Al	1.21	1.21	1.17	1.13	1.14	1.15	1.15	1.11				
Fe	0.00	0.00	0.00	0.00	0.00	0.00	0.00	0.00	Total	8.00	8.00	8.00
Mn	0.00	0.00	0.00	0.00	0.00	0.00	0.00	0.00				
Na	0.73	0.77	0.76	0.83	0.82	0.80	0.80	0.85	Al(VI)	2.69	2.74	2.82
K	0.02	0.01	0.00	0.00	0.00	0.01	0.01	0.00	Fe^{2+}	4.92	4.60	4.85
Mg	0.00	0.00	0.00	0.00	0.00	0.00	0.00	0.00	Mg	4.22	4.53	4.08
Ca	0.21	0.20	0.17	0.14	0.14	0.15	0.18	0.12	Mn	0.06	0.05	0.07
Ti	0.00	0.00	0.00	0.00	0.00	0.00	0.00	0.00				
Cr	0.00	0.00	0.00	0.00	0.00	0.00	0.00	0.00	Total	11.89	11.91	11.82
Total	4.97	4.98	4.95	4.97	4.97	4.97	4.98	4.97	XFe	0.54	0.50	0.54
AB	76.46	78.66	81.66	85.15	85.17	83.58	81.30	87.57				
OR	1.63	1.09	0.47	0.40	0.42	0.53	0.59	0.30				
AN	21.91	20.25	17.87	14.44	14.41	15.89	18.11	12.13				

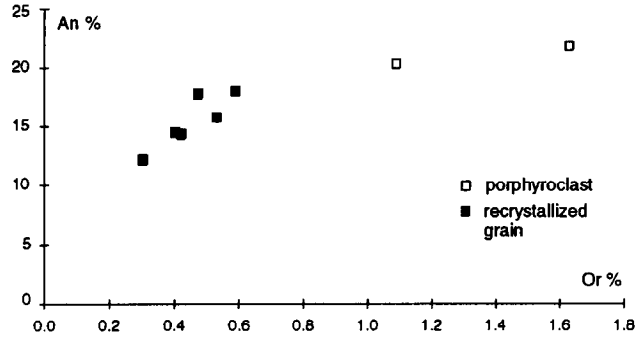

Fig. 5. Relation between anorthite and K-feldspar components in non-recrystallized (open square) and recrystallized (solid square) plagioclase of the sheared dike.

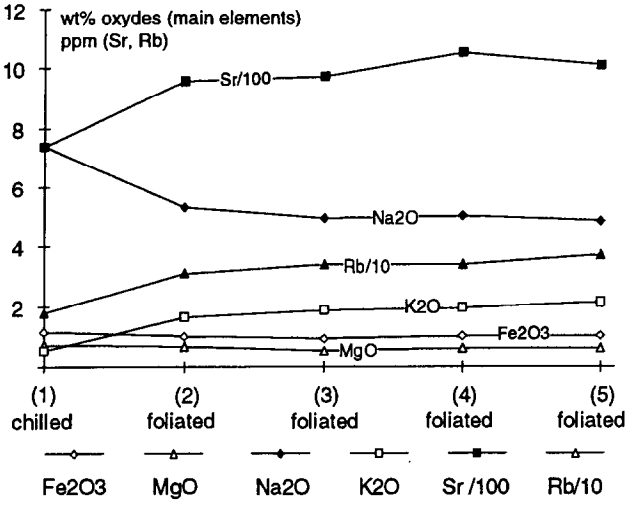

Fig. 6. Geochemical data of the trondhjemitic dike. Note the change in composition from the chilled margin (zone 1) to the central parts of the dike (zones 2 to 5).

dikes are similar (Vejnar, 1984), (2) the trondhjemites are cut by late Cambrian to early Ordovician pegmatites, (3) in the quarry U baldovske Kaple (north of Domažlice), the trondhjemitic dikes are affected by Variscan thrusts and folds. Rb–Sr whole rock and K–Ar dating of white mica of the dike yield ages between 362 and 371 Ma (Wemmer and Ahrendt, pers. commun.). These ages are comparable with those of the adjacent metasediments of the Domažlice area and thus are interpreted as cooling ages. They clearly indicate that the K–Ar and Rb–Sr isotopic systems were still open during the Variscan cycle. This is compatible with the greenschist facies conditions described above for the Variscan event.

Microfabrics and deformation mechanisms

The fine-grained chilled margin can be further subdivided under the microscope. A completely isotropic narrow zone of 0.3 mm wide occurs along the contact to the wall rock (Fig. 3e). The remaining part of the chilled margin has a faint, but distinct, foliation marked by the weak shape-preferred orientation of rare biotites, and of zoned plagioclase grains up to 300 μm in size. Most plagioclase and quartz grains of the chilled margin are dynamically recrystallized with recrystallized grains of less than 50 μm in size.

Towards the centre of the dike a strongly foliated zone, ca 5 mm in width, appears where biotite is the only mica phase. Although plagioclase porphyroclasts are more frequent than in the chilled margin, most of them are completely recrystallized.

The central part of the dike is not very different from the marginal biotite-bearing zone except that, instead of biotite, muscovite is the dominant mica phase. Rare biotite is restricted to small inclusions within primary grains of plagioclase as well as to streaked clusters of biotite. Frequently observed pseudomorphs of muscovite after biotite suggest that biotite was the primary (magmatic) phase. The pseudomorphs can be easily recognized by plates of ilmenite that decorate the cleavage planes of the new muscovite. Other muscovite grains, free from ilmenite, grew at the expense of plagioclase, thus increasing the mica content of the central part of the dike up to more than 20%. All muscovites show a strong shape-preferred orientation that, together with the dynamically recrystallized plagioclase and quartz grains, contributes to the mylonitic foliation.

Microscopic shear sense indicators are rare in the central part of the dike. In a few cases we observed weakly developed shear bands and asymmetric pressure shadows of recrystallized plagioclase and muscovite on plagioclase porphyroclasts (σ clasts) confirming the macroscopically derived dextral displacement sense.

Strain analysis

Since quartz and plagioclase are strongly recrystallized, both minerals cannot be used to determine the finite strain of the dike. Randomly oriented micas of igneous origin are generally suitable 'passive' markers for measuring the strain within deformed magmatic rocks (March, 1932). As the narrow zone at the very contact to the wall rock shows almost no preferred orientation of biotite and plagioclase phenocrysts, a magmatic foliation probably did not exist in the dike before the subsolidus shearing occurred. This is also confirmed by the non-foliated porphyritic trondhjemitic dikes of the Domažlice area that do not display a shape-preferred orientation of micas due to magmatic flow.

To determine the strain of the trondhjemitic dike is complicated by the fact that the micas formed at different stages during the cooling of the magma (see above). Biotite of the chilled margin and adjacent domains represents the magmatic mica phase, the shape of which was hardly affected during subsequent shearing. Biotite is therefore most appropriate for measuring early strain increments. The white micas at the centre of the dike, that grew during the subsolidus shearing at the expense of

plagioclase and biotite, should reflect only the late increments of the bulk strain.

To measure the strain of the dike, we applied the image analysis system DIAna developed by Duyster (1991), which includes the procedure 'Partikelprojektions-methode' that measures strain by the SURFOR method (see Panozzo, 1984). We assumed that the particles (micas) did not vary in shape during deformation. As the SURFOR technique, analogous to the theory of March (1932), assumes that deformation is homogeneous including the change in length of the particles (lines), the strain determined by this method does not reflect the real strain. The 'real' strain was obtained from the SURFOR strain as follows. By means of a vector graphics program, we homogeneously 'deformed' a square area by simple shear. The square contains a circle, used as strain marker, and randomly oriented segments that change in length and orientation during the 'deformation'. The SURFOR strain of the deformed square, determined by measuring the orientation and length of the lines with the 'Partikel-projektionsmethode', is similar to the strain derived from the strain ellipse inscribed in the deformed square. The square was incrementally deformed, and in every state of finite strain the change in length of all lines was cancelled while their orientation was retained. The real strain of the revised object is here referred to as the 'modified SURFOR strain'. When plotted against the SURFOR strain (ϵ_S) in a X–Y diagram, the modified SURFOR strain (ϵ_R) varies almost linear according to the equation:

$$\epsilon_R = 2.1 \times \epsilon_S - 1.25. \quad (1)$$

This equation was applied to the strain data determined with the 'Partikelprojektionsmethode' to calculate the real strain.

We measured about 3500 micas on X–Z and Y–Z thin sections. As primary biotite is largely preserved in the marginal part of the dike, the latter was divided into 4 distinct zones (each 0.5 cm wide) oriented parallel to the dike boundary. Each of these zones was studied separately. The inset in Fig. 7 shows the increase in length of the micas from the chilled margin (zone 1) towards the central parts (zones 2 to 4). The chilled margin and the adjacent zone 2 contain magmatic biotite, whereas the remaining zones (3 and 4) contain secondary white mica. On the Flinn graph, the strain data of every zone, depicted as rhombs, plot within the apparent constrictional field (Fig. 7). However, the strain intensity increases considerably from the chilled margin ($e_X = 1.7$) to zone 4 ($e_X = 2.6$).

The influence of a possible volumetric strain on the finite strain ellipsoid (Ramsay and Wood, 1973) was investigated using the geochemical method of Grant (1976). The concentrations of immobile elements (Zr, Ti, Nb, Al) of the almost non-altered chilled margin (zone 1) were plotted against those of the strongly altered part of the dike (zones 2 to 4) (Fig. 8). As the immobile elements do not significantly vary, a volumetric strain

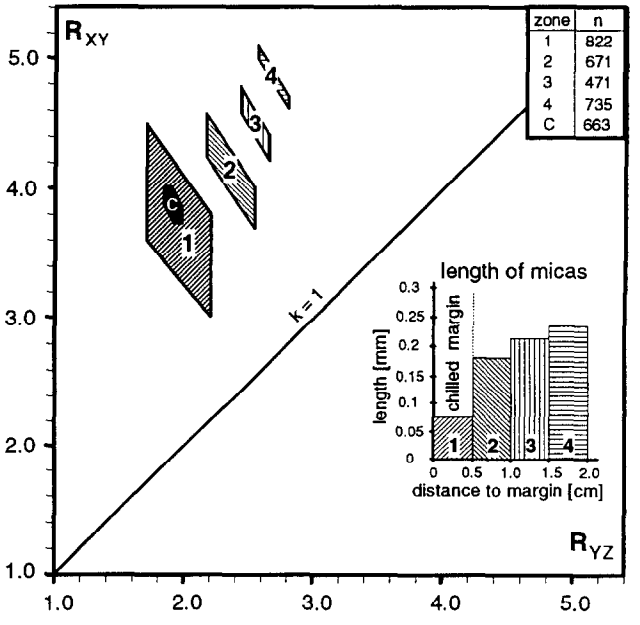

Fig. 7. Flinn graph showing the strain geometry in the chilled margin (1) and adjacent marginal zones of the trondhjemitic dike (2–4) determined by the SURFOR method (see text). Black field (C) denotes the strain in the central part of the dike. The inset gives the increase of mica length from the chilled margin towards the centre of the dike (mean values).

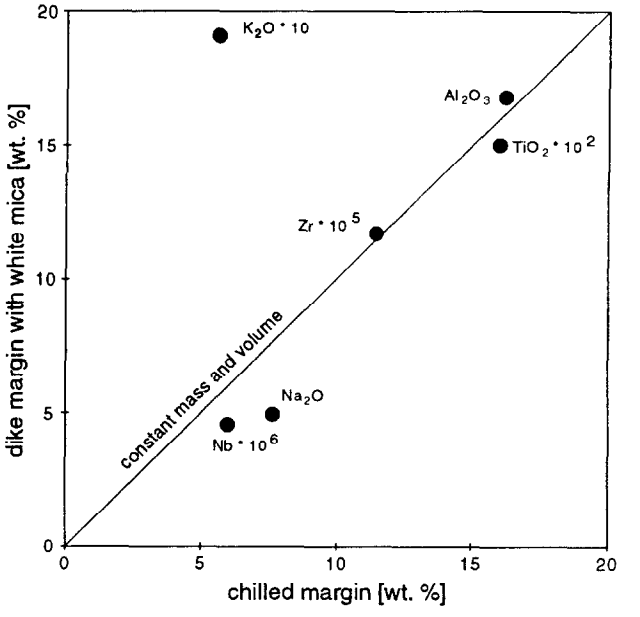

Fig. 8. Grant (1976) diagram showing the content of immobile elements in the chilled margin (zone 1) and adjacent marginal zones (2 to 5) of the dike.

should be ruled out for the altered parts of the dike. Thus, the apparent constrictional strain determined above should reflect the actual state of strain.

The apparent constrictional strain makes it difficult to determine the shear strain of the dike and its relation to the longitudinal strain. To simplify the calculation, we

assumed simple shear, being aware that the results may deviate from those expected from apparent constrictional conditions. Assuming simple shear, the shear strain (γ) can be determined from the angle between the S and C planes of the shear zone

$$\gamma = 2/\tan 2\theta' \quad (2)$$

where θ' is the acute angle between the S and C planes (see Ramsay and Graham, 1970). In the present case, θ' ranges from 10° to 15° (Fig. 3g) yielding a shear strain between 3.5 and 5.5. In simple shear, the longitudinal strain along the major principal axis of the finite strain ellipsoid (e_X) is approximately half the value of the shear strain (Pfiffner and Ramsay, 1982). In the present case, the longitudinal strain, calculated from the shear strain, ranges from 1.8 to 2.9. Thus, although the prerequisites for the above calculations are not entirely fulfilled because of the deviation from simple shear, the calculated longitudinal strain is approximately compatible with the modified SURFOR strain (1.7–2.6) determined by applying the 'Partikelprojektionsmethode' described above.

Finally, it has to be noted that the strain magnitude of the central part of the dike (C in Fig. 7) is as low as that of the chilled margin.

THERMAL MODELLING

The thermal history of the dike and its surroundings has been numerically simulated assuming a temperature of 350°C for the wall rock. The temperature of the intruding trondhjemitic melt was determined applying the zircon saturation method of Watson and Harrison (1983). As the chilled margin of the trondhjemitic dike hardly shows post-magmatic chemical and mineralogical alteration, it is the most suitable candidate for carrying out this calculation. Taking into account the cation ratio and Zr content (114 ppm) of the chilled margin, a temperature of 750°C was determined. Since no zircon could be found in the dike, the amount of inherited zircons should be low. Consequently, the temperature determined should approximately reflect the temperature of the melt (Watson and Harrison, 1986). It has to be further emphasized that calculations of the melt temperature of the large Mračnice trondhjemite and of several non-foliated porphyritic trondhjemitic dikes yield nearly the same values as that of the foliated dike described here.

Calculations with the FUSION program of Niederkorn and Blumenfeld (1989) suggest that, under water-saturated conditions, a tonalitic melt can be expected to include about 50% crystals at a temperature of 750°C, and the solidus should be close to 650°C (Bouchez *et al.*, 1992) (Fig. 9). The relatively high amount of An in the magmatic plagioclase of the trondhjemitic dike (Fig. 5) suggests that the composition of the dike is close to that

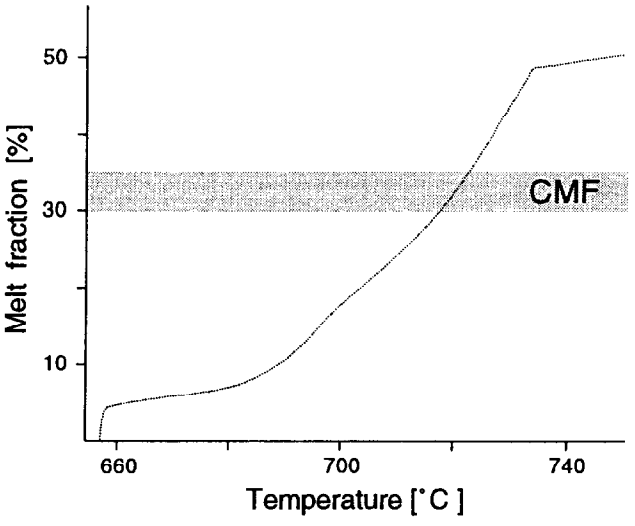

Fig. 9. Melting curve of a tonalite under water-saturated conditions (after Bouchez *et al.*, 1992). CMF = critical melt fraction.

of a tonalite (see An–Ab–Or diagram of Barker, 1979). Hence, we adopt the data of the tonalite by setting the temperature interval of crystallisation of the trondhjemitic dike at 100°C.

The heat of fusion was also taken at 100°C, i.e. half the value for felsic melts (see Peacock, 1989). Fifty percent of crystals already existed when the melt emplaced. The thermal conductivity was set at 2.63 $W\,m^{-1}\,K^{-1}$, and the heat capacity was assumed to be 1 $kJ\,kg^{-1}\,K^{-1}$ (Čermák *et al.*, 1982). From the results of the XRD analyses, the density of the dike was set at 2663 $kg\,m^{-3}$, and for the sake of simplicity, the heat was assumed to be transported by conduction only, and the width of the dike was fixed at 1 m.

The numerical simulation was carried out with the program 'CONTACT' (Peacock, 1989) based on a finite difference algorithm to solve the one-dimensional heat transfer equation. It assumes that the igneous body intrudes instantaneously. This should be the case for the trondhjemitic dike, since the chilled margin of the dike as well as the absence of significant contact heating of the wall rock clearly indicate a single-stage fast intrusion (see Jaeger, 1968, p. 516; Clemens and Mawer, 1992).

Figure 10(a) shows a temperature vs distance plot where the calculated isotherms within the dike and country rock are depicted for time-steps of 1 day. Figure 10(b) shows the maximum temperature achieved at each point during, and subsequent to, the magmatic event. Finally, in a time vs temperature plot (Fig. 10c) the temperature–time path is given for 5 points located at distances of −0.5 m (centre of the dike), −0.25 m, 0 m (dike/wall rock boundary), +0.25 m and +0.5 m. In the following section we will focus on three distinct temperatures critical for the rheology of the dike during its deformation: (1) the temperature of the rheologically critical melt fraction (CMF = 30–35% melt, Van der Molen and Paterson, 1979), which in our case is around

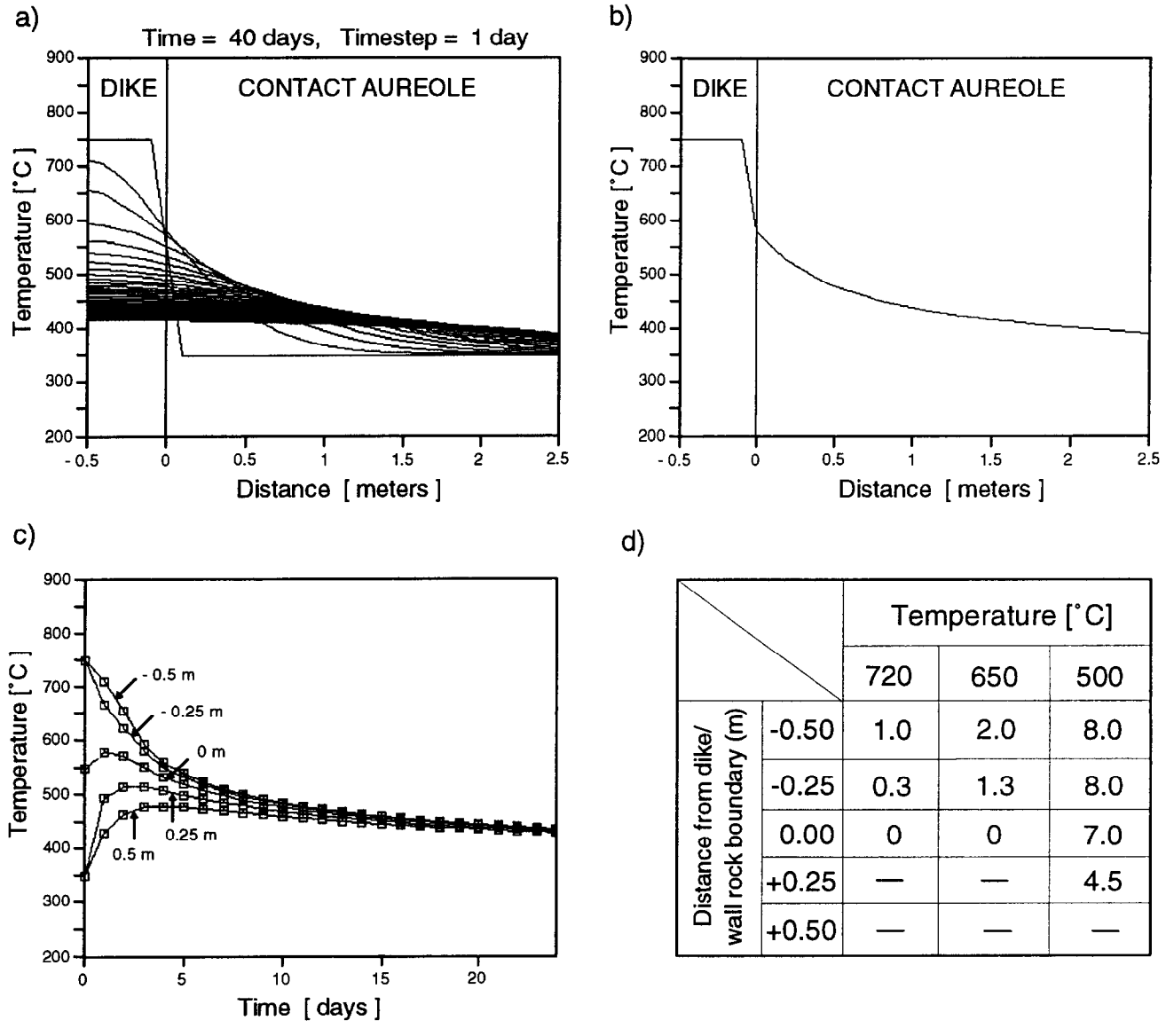

Distance from dike/wall rock boundary (m)	Temperature [°C] 720	650	500
-0.50	1.0	2.0	8.0
-0.25	0.3	1.3	8.0
0.00	0	0	7.0
+0.25	—	—	4.5
+0.50	—	—	—

Fig. 10. Thermal modelling carried out with the program CONTACT of Peacock (1989). (a) Temperature vs distance plot showing the temperature profiles for 40 days (each curve = 1 day); the steepest curve represents the temperature profile at the moment of melt emplacement; for symmetry reasons only half the dike is shown. (b) Temperature vs distance plot showing the maximum temperature at each point achieved during and subsequent to the intrusion. (c) Temperature vs time plot showing the temperature–time paths at different distances from the centre of the dike. (d) Cooling time (in days) to reach rheologically critical temperatures at different distances (in meters) from the dike centre. Further explanation in text.

720°C (Fig. 9); (2) the solidus temperature (650°C; Fig. 9); and (3) the threshold temperature for the onset of pervasive crystal plastic deformation by recrystallization-accomodated dislocation climb of plagioclase, i.e. approximately 500°C for plagioclase that is poor in An component and at natural strain rates (Voll, 1976; Tullis and Yund, 1991; Pryer, 1993).

At the dike/wall rock contact, where the chilled margin developed and at $t = 0$, the temperature does not exceed 550°C (Fig. 10a). Due to the latent heat of crystallization, the temperature slightly increased up to a maximum value of 580°C after 1.25 days. Then, the temperature decreased down to 500°C after 7 days.

At the centre of the dike (Fig. 10 a & b) a temperature of $T = 720$°C was realized after about 1 day. The solidus temperature ($T = 650$°C) was reached after 2 days, and $T = 500$°C after 8 days. Regarding the country rock, $T = 500$°C was never reached at a distance of more than +0.4 m away from the dike (Fig. 10b), and at +2.5 m the maximum temperature was $T = 380$°C.

DISCUSSION

Structural and microstructural data, presented in this paper, indicate the syn-emplacement deformation of a trondhjemitic dike. Intrusion of the dike into an active shear zone is documented by the following facts:

(1) the structural elements, shear plane, stretching lineation, and the sense of shear are concordant in the dike and country-rock;

(2) plagioclase was strongly recrystallized in the dike, including its foliated chilled margin, but not in the country rock; this indicates that the temperature within the dike exceeded that of the country rock during ductile deformation;

(3) pervasive recrystallization of plagioclase and quartz in the dike contributes to a 'high-temperature' foliation that is considerably stronger than in the sheared country rock;

(4) the degree of retrograde metamorphism is much weaker in the country-rock close to the dike (< 0.5 m), than farther away from it, indicating a slight contact heating during shearing;

(5) the major glide systems in quartz of the country-rock change significantly from the basal $<a>$ glide to rhombohedral and prism $<a>$ glide when approaching the dike; this also indicates that the temperature increased during shearing when approaching the dike.

Thermal modelling suggests that the rheology of the dike must have changed significantly within about 8 days. Figure 11 shows how, during cooling, the high-viscosity zone migrates from the margins of the dike towards its centre. After 12 h of cooling, the amount of melt in the centre of the dike was still above the rheological critical melt fraction (30–35%), meaning that this part of the dike behaved as a melt with approximately Newtonian properties. The margins of the dike were already below the solidus temperature, but the plagioclase could still recrystallize. The amounts of melt in-between the centre and the margin of the dike were below the CMF. Thus, analogous to the margin, this part of the dike behaved like a solid. After 1 day of cooling, the entire dike behaved as a solid, i.e. $T < 720$°C, and after 2 days, remnants of melt were restricted to the very centre of the dike. During the following 3 to 6 days after melt emplacement, the entire dike was in a subsolidus state, i.e. at temperatures in-between 650 and 500°C where plagioclase could still recrystallize. After 7 days the temperature at the margins was less than 500°C. Consequently, plagioclase should behave brittlely. After 8 days, the whole dike was in a state where plagioclase is expected to deform by fracturing. Hence, recrystallization of plagioclase should have been restricted to a time interval of about 8 days after the melt was emplaced. If the threshold temperature for recrystallization of plagioclase is lower, say 450°C, this critical time interval increases to 16 days.

It is emphasized that the chilled margin became a solid instantaneously. Nevertheless, during the first 7 days, the temperature was high enough for recrystallization of quartz and plagioclase. Thus, the rheological contrast within the chilled margin was markedly low supporting pervasive and fully ductile deformation during the shearing event. Taking into account the magnitude of finite strain as well as the maximum possible time that was necessary for imposing this strain, we are able to calculate the strain rate of the shearing event. Since the chilled margin yields reliable strain data, it is suitable to carry out such a calculation. There are several reasons for why the major part of the strain in the chilled margin should have developed within the first 7 days:

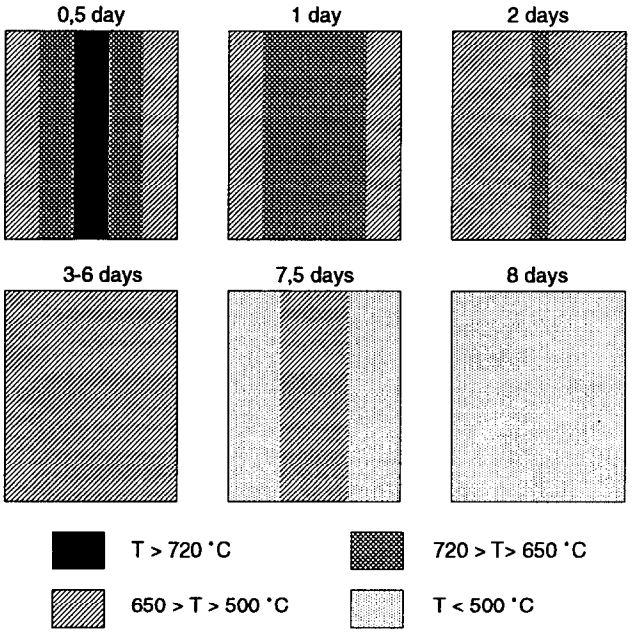

Fig. 11. Sketches showing the time-dependent change in distribution of temperature, and hence of rheologically distinct domains. Black area = $T > 720$°C: melt content is above the rheologically critical melt fraction; dark grey area = 650°C < T < 720°C: melt is present but in amount below the rheologically critical fraction; grey area = 500°C < T < 650°C: solidus is reached but temperature was high enough for plagioclase recrystallization; light grey area = $T < 500$°C: plagioclase does not recrystallize.

(1) plagioclase behaved exclusively by crystal plastic deformation suggesting a temperature higher than ca 500°C;

(2) in contrast to the centre of the dike, magmatic biotite and plagioclase phenocrysts were not replaced by white mica in the rim;

(3) the low amounts of quartz within the chilled margin (25%) are probably not sufficient to weaken the plagioclase-controlled shear zone by its shape-preferred orientation at temperatures lower than about 500°C (Handy, 1990).

In the chilled margin the longitudinal strain along X is $e_X = 1.7$. If this strain was imposed within the first 7 days after the dike emplaced, the average strain rate would be $2.8 \times 10^{-6}\ s^{-1}$, equivalent to a displacement rate of 2 cm h^{-1}. This strain rate is several orders of magnitudes higher than geological strain rates given in the literature. The large amount of data compiled by Pfiffner and Ramsay (1982) suggest that geological strain rates commonly range from 1×10^{-13} to $1 \times 10^{-15}\ s^{-1}$. In high-strain domains, like shear zones, these values may

reach values up to $1 \times 10^{-10}\,s^{-1}$ (Carter and Tsenn, 1987 and references therein). Concerning emplacement-related deformation of granitoid magmas, John and Blundy (1993) calculated a strain rate of 4 to $13 \times 10^{-13}\,s^{-1}$ for granitoids of the Adamello Massif of the Italian Alps. A higher strain rate of 1×10^{-11} to $1 \times 10^{-12}\,s^{-1}$ was derived by Karlstrom *et al.* (1993) from a synkinematic pluton of the Piute Mountains (southern California).

We explain the extremely high strain rate, derived from the chilled margin of the trondhjemitic dike, as the result of local strain accumulation supported by the 'lubricating' melt (see Arzi, 1978; Hollister and Crawford, 1986; Karlstrom *et al.*, 1993). Regarding the whole dike, this strain rate is probably a minimum strain rate, since:

(1) the thermal modelling does not consider advective heat transported by circulating fluids that probably increased the cooling rate of the dike, hence increasing the strain rate;

(2) the higher amounts of melt in the centre of the dike weakened this part of the dike compared with the solid marginal parts where the strain and strain rate should be lower;

(3) the assumed time interval of 7 days should be treated as a maximum value, because the chilled margin may have been strained in a time interval that is considerably smaller.

The latter point is particularly important. Taking the results of experimental deformation of plagioclase into account, the high strain rate determined above is hardly compatible with crystal plastic deformation of plagioclase. At a strain rate of $10^{-6}\,s^{-1}$, recrystallization-accomodated dislocation climb of An-poor plagioclase should be possible only at temperatures above 700°C under dry conditions (Tullis and Yund, 1991; Fig. 7a). Below this temperature, cataclastic flow should be expected. This suggests that the time interval for plagioclase recrystallization shrinks to a few hours, and this would further increase the strain rate. The question arises of whether the experimental results apply to our case. The experiments, for example, do not consider the presence of a melt phase from which plagioclase crystallized. Under wet deformation conditions, on the other hand, diffusion creep and grain boundary sliding should be the prevailing deformation mechanisms at a strain rate of $10^{-6}\,s^{-1}$ and $T < 700$°C (Tullis and Yund, 1991; Fig. 7b). Since evidence for pervasive diffusion creep is lacking in the chilled margin, relatively dry conditions must be assumed during the initial shearing phase.

It is difficult to interpret the strain data of the central part of the dike. Replacement of large amounts of plagioclase by white mica decreased the plagioclase content from 72% (chilled margin) to 48%, and increased the mica content from 2% (chilled margin) to 20%. These fluid-assisted mineralogical and textural changes should have contributed to significant strain softening in the central part of the dike. This holds also for temperatures lower than 500°C. It cannot be excluded that, in the central part of the dike, a considerable part of the late-stage displacement was accommodated by the weak phases (mica and quartz). Thus, the deformation may have continued within the brittle regime of plagioclase, although the latter does not show evidence for pervasive fracturing and cold working. It is assumed that these processes may have contributed to a more homogeneous strain in the central part of the dike as is indicated by the weak scattering of the data points in the Flinn diagram.

There are two reasons to interpret the markedly low strain in the central part of the dike as a minimum strain: (1) the white micas grew late in the deformation history and do not record the bulk strain; and (2) the displacement in the central part of the dike may have initially occurred under magmatic conditions.

CONCLUSIONS

Our results clearly show that synkinematically intruded dikes may display significant lateral zonations in strain, mineralogy and geochemistry. These zonations are interpreted as the result of the time-dependent shift in rheological conditions of the cooling dike from its margins to its centre. The shift in the rheological state goes in concert with a shift in the intensity of deformation. Subsolidus strain occurred first in the chilled margin of the investigated trondhjemitic dike and was shifted from there towards its centre. As the subsolidus deformation 'migrated' towards the weak centre of the dike, the rigid chilled margin was prevented from further deformation, and its strain was 'frozen'. The fact that fluid-controlled alteration is restricted to the central parts of the dike suggests that a migrating fluid front appeared late during the shearing event and thus post-dated the intrusion of the melt. Although shearing of the dike was approximately volume-constant, the fluids contributed to a significant exchange in sodium and potassium, whereas the amount of other main elements did not markedly change. We believe that similar synkinematic dikes may be present in other areas of active magmatism, particularly in regions with active volcanism. The extremely high strain rate, derived from the chilled margin of the trondhjemitic dike, is probably not an exception. However, the prerequisites for calculating strain rates of synkinematic dikes are rarely given in nature.

Acknowledgements—We thank J. L. Bouchez, C. W. Passchier and an anonymous reviewer for numerous helpful criticisms and suggestions that considerably improve the quality of this paper. We are further grateful to Z. Vejnar and J. Fiala who provided invaluable help in the field. Thanks also to A. Hoffmann (Gießen) who carried out the XRF and XRD analyses. Further, we thank J. Schumacher (Freiburg) and R. Petschick (Frankfurt) for their help to carry out the thermal modelling. The microprobe analyses of chlorite were accomplished by S. Büttner who is gratefully acknowledged. This study was financially supported by the Deutsche Forschungsgemeinschaft (SPP 'Orogene Prozesse: ihre Quantifizierung und Simulation am Beispiel der Varisciden', grant No. Zu 73/1-3).

REFERENCES

Aranguren, A. and Tubia, J. M. (1992) Structural evidence for the relationship between thrusts, extensional faults and granite intrusions in the Variscan belt of Galicia (Spain). *Journal of Structural Geology* **14**, 1229–1237.

Arzi, A. (1978) Critical phenomena in the rheology of partially melted rocks. *Tectonophysics* **44**, 173–184.

Barker, F. (1979) Trondhjemites: definition, environment and hypotheses of origin. In *Trondhjemites, Dacites and Related Rocks*, ed. F. Barker, pp. 1–12. Elsevier, Amsterdam.

Berthé, D., Choukroune, P. and Jegouzo, P. (1979) Orthogneiss, mylonite and non-coaxial deformation of granites: the example of the South Armorican Shear Zone. *Journal of Structural Geology* **1**, 31–42.

Bouchez, J. L., Delas, C., Gleizes, G., Néd, A. and Cuney, M. (1992) Submagmatic microfractures in granites. *Geology* **20**, 35–38.

Bouchez, J. L. and Pecher, A. (1981) The Himalayan main central thrust pile and its quartz-rich tectonites in central Nepal. *Tectonophysics* **78**, 23–50.

Carter, N. L. and Tsenn, M. C. (1987) Flow properties of continental lithosphere. *Tectonophysics* **136**, 27–63.

Castro, A. (1987) On granitoid emplacement and related structures. A review. *Geologische Rundschau* **76**, 101–124.

Castro, A., De la Rosa, J. D., Fernández, C. and Moreno-Ventas, I. (1995) Unstable flow, magma mixing and magma-rock deformation in a deep-seated conduit: the Gil-Márquez Complex, south-west Spain. *Geologische Rundschau* **84**, 359–374.

Cathelineau, M. (1988) Cation site occupancy in chlorites as a function of temperature. *Clay Mineralogy* **23**, 471–485.

Cathelineau, M. and Nieva, D. (1985) A chlorite solution geothermometer. The Los Azufres (Mexico) geothermal system. *Contributions to Mineralogy and Petrology* **91**, 235–244.

Čermák, V., Huckenholz, H.-G., Rybach, L., Schmid, R., Schopper, J. R., Schuch, M., Stöffler, D. and Wohlenberg, J. (1982) Physical properties of rocks. In *Landolt–Börnstein, Numerical Data and Functional Relationships in Science and Technology, Group V: Geophysics and Space Research*, ed. H. Angenheister, pp. 305–370. Springer-Verlag, Berlin.

Chlupáč, J. (1993) *Geology of the Barrandian. A Field Trip Guide.* Waldemar Kramer, Frankfurt a.M.

Clemens, J. D. and Mawer, C. K. (1992) Granitic magma transport by fracture propagation. *Tectonophysics* **204**, 339–360.

Dörr, W., Fiala, J., Philippe, S., Vejnar, Z. and Zulauf, G. (1995) Cadomian vs Variscan imprints in the Teplá-Barrandian unit, Part A: U–Pb ages of pre-Variscan granitoids. *Terra nostra* **95/8**, 91.

Duyster, J. (1991) Strukturgeologische Untersuchungen im Moldanubikum (Waldviertel, Österreich) und methodische Untersuchungen zur bildanalytischen Gefügequantifizierung von Gneisen. Ph.D. thesis, Universität Göttingen.

Emerman, S. H. and Marrett, R. (1990) Why dikes? *Geology* **18**, 231–233.

Glodny, J., Grauert, B., Krohe, A., Vejnar, Z. and Fiala, J. (1995) Altersinformation aus Pegmatiten der westlichen Böhmischen Masse: ZEV, Teplá-Barrandium und Moldanubikum. *8. DFG-Kolloquium SPP Kontinentales Tiefbohrprogramm der Bundesrepublik Deutschland, 25.-26.5.1995*, Gießen (abstract).

Grant, J. A. (1976) A simple solution to GRESENS' equation for metasomatic alteration. *Economic Geology* **81**, 1976–1982.

Guineberteau, B., Bouchez, J. and Vigneresse, J. (1987) The Mortagne granite pluton (France) emplaced by pull-apart along a shear zone: Structural and gravimetric arguments and regional implications. *Bulletin of the Geological Society of America* **99**, 763–770.

Handy, M. R. (1990) The solid-state flow of polymineralic rocks. *Journal of Geophysical Research* **95**, 8647–8661.

Hippertt, J. F. (1994) Microstructures and *c*-axis fabrics indicative of quartz dissolution in sheared quartzites and phyllonites. *Tectonophysics* **229**, 141–163.

Hoeppener, R. (1955) Tektonik im Schiefergebirge. *Geologische Rundschau* **44**, 26–58.

Hollister, L. S. and Crawford, M. L. (1986) Melt-enhanced deformation: A major tectonic process. *Geology* **14**, 558–561.

Hudec, M. R. (1992) Mesozoic structural and metamorphic history of the Central Ruby Mountains metamorphic core complex, Nevada. *Bulletin of the Geological Society of America* **104**, 1086–1100.

Hutton, D. H. W. (1988) Igneous emplacement in a shear zone termination: the biotite granite at Strontian, Scotland. *Bulletin of the Geological Society of America* **100**, 1392–1399.

Hutton, D. H. W. (1992) Granite sheeted complexes: evidence for the dyking ascent mechanism. *Transactions of the Royal Society, Edinburgh* **83**, 377–382.

Hutton, D. H. W., Dempster, T. J., Brown, P. E. and Becker, S. D. (1990) A new mechanism of granite emplacement: Intrusion in active extensional shear zones. *Nature* **343**, 452–455.

Hutton, D. H. W. and Reavy, R. J. (1992) Strike-slip tectonics and granite petrogenesis. *Tectonics* **11**, 960–967.

Ingram, G. M. and Hutton, D. H. W. (1994) The Great Tonalite Sill: Emplacement into a contractional shear zone and implications for Late Cretaceous to early Eocene tectonics in southeastern Alaska and British Columbia. *Bulletin of the Geological Society of America* **106**, 715–728.

Jaeger, J. C. (1968) Cooling and Solidification of Igneous Rocks. In *Basalts: The Poldervaart Treatise on Rocks of Basaltic composition*, eds H. H. Hess and A. Poldervaart, Vol. 2, pp. 503–536. Interscience Publishers, New York.

John, B. E. and Blundy, J. D. (1993) Emplacement-related deformation of granitoid magmas, southern Adamello Massif, Italy. *Bulletin of the Geological Society of America* **105**, 1517–1541.

Jowett, E. C. (1991) Fitting iron and magnesium into the hydrothermal chlorite geothermometer.—GAC/AGC-MAC/AMC—*SEG, Program with Abstracts* **16**, A62.

Karlstrom, K. E., Miller, C. F., Kingsbury, J. A. and Wooden, J. L. (1993) Pluton emplacement along an active ductile thrust zone, Piute Mountains, southeastern California: Interaction between deformational and solidification processes. *Bulletin of the Geological Society of America* **105**, 213–230.

Karlstrom, K. E. and Williams, M. L. (1995) The case for simultaneous deformation, metamorphism and plutonism: an example from Proterozoic rocks in central Arizona. *Journal of Structural Geology* **17**, 59–81.

Košler, J., Rogers, G., Bowes, D. R. and Hopgood, A. M. (1994) Rb–Sr isotopic evidence for polymetamorphism in the Domažlice crystalline complex from a study of mica-feldspar pairs in a segregation pegmatite near Stráž, western Bohemia. *Mitt. Öster. Miner. Ges.* **139**, 75–76.

Kreuzer, H., Müller, P., Okrusch, M., Patzak, M., Schüssler, U., Seidel, E., Šmejkal, V. and Vejnar, Z. (1990) Ar–Ar confirmation for Cambrian, early Devonian and mid-Carboniferous tectonic units at the western margin of the Bohemian Massif. *6. Rundgespräch Geodynamik des Europ. Variszikums; 15.–18.11.1990*; Clausthal–Zellerfeld (abstract).

Krohe, A. (1990) Local variations in quartz [*c*]-axis orientation in noncoaxial regimes and their significance for the mechanics of *S–C* fabrics. *Journal of Structural Geology* **12**, 995–1004.

Lister, G. S. and Baldwin, S. L. (1993) Plutonism and the origin of metamorphic core complexes. *Geology* **21**, 607–610.

Lister, G. S. and Williams, P. F. (1979) Fabric development in shear zones: theoretical controls and observed phenomena. *Journal of Structural Geology* **1**, 283–297.

March, A. (1932) Mathematische Theorie der Regelung nach der Korngestalt bei affiner Deformation. *Z. Kristallogr.* **81**, 285–297.

Niederkorn, R. and Blumenfeld, P. (1989) FUSION: A computer simulation of melting in the Quartz–Albite–Anorthite–Orthoclase system. *Computers and Geosciences* **15**, 347–369.

Nyman, M. W., Karlstrom, K. E., Kirby, E. and Graubard, C. M. (1994) Mesoproterozoic contractional orogeny in western North America: Evidence from ca 1.4 Ga plutons. *Geology* **22**, 901–904.

Panozzo, R. (1984) Two dimensional strain from the orientation of lines in a plane. *Journal of Structural Geology* **6**, 215–221.

Parsons, T. and Thompson, G. A. (1993) Does magmatism influence low-angle normal faulting? *Geology* **21**, 247–250.

Paterson, S. R. and Fowler, K. (1993) Re-examining pluton emplacement processes. *Journal of Structural Geology* **15**, 191–206.

Paterson, S. R. and Tobisch, O. T. (1988) Using pluton ages to date regional deformation: problems with present criteria. *Geology* **16**, 1108–1111.

Paterson, S. R. and Tobisch, O. T. (1992) Rates of processes in magmatic arcs: implications for the timing and nature of pluton emplacement and wall rock deformation. *Journal of Structural Geology* **14**, 291–300.

Peacock, S. M. (1989) Thermal modeling of metamorphic pressure–temperature–time paths: a forward approach. In *Metamorphic Pressure–Temperature–Time Paths*, eds F. S. Spear and S. M. Peacock,

Vol. 7, pp. 57–102. American Geophysical Union, Short Course in Geology.

Petford, N., Ker, R. C. and Lister, J. R. (1993) Dike transport of granitoid magmas. *Geology* **21**, 845–848.

Pfiffner, O. A. and Ramsay, J. G. (1982) Constraints on geological strain rates: arguments from finite strain states of naturally deformed rocks. *Journal of Geophysical Research* **87**, 311–321.

Pryer, L. L. (1993) Microstructures in feldspars from a major crustal thrust zone: the Grenville Front, Ontario, Canada. *Journal of Structural Geology* **15**, 21–36.

Ramsay, J. G. and Graham, R. H. (1970) Strain variations in shear belts. *Canadian Journal of Earth Sciences* **7**, 786–813.

Ramsay, J. G. and Wood, D. S. (1973) The geometric effects of volume change during deformation processes. *Tectonophysics* **16**, 263–277.

Sleep, N. H. (1988) Tapping of melt by veins and dikes. *Journal of Geophysical Research* **B93**, 10255–10272.

Šmejkal, V. and Vejnar, Z., (1967) Zur Frage des praevaristischen Alters einiger Granitoide des Böhmischen Massivs. *Sbornik I. Geochemical Conference*, Ostrava, 1965.

Spence, D. A. and Turcotte, D. L. (1985) Magma-driven propagation of cracks. *Journal of Geophysical Research* **B90**, 575–580.

Suppe, J. (1985) *Principles of Structural Geology*. Prentice-Hall, New Jersey.

Tonika, J. and Vejnar, Z. (1966) Geologie a petrografie stodskeho masivu. *Časopis pro mineralogii a geologii* **25**, 129–137.

Tullis, J., Christie, J. M. and Griggs, D. T. (1973) Microstructures and preferred orientations of experimental deformed quartzites. *Bulletin of the Geological Society of America* **84**, 297–314.

Tullis, J. A. and Yund, R. A. (1991) Diffusion creep in feldspar aggregates: experimental evidence. *Journal of Structural Geology* **13**, 987–1000.

Van der Molen, I. and Paterson, M. S. (1979) Experimental deformation of partially melted granite. *Contributions to Mineralogy and Petrology* **70**, 299–318.

Vejnar, Z. (1982) Regionální metamõrfoza psamiticko-pelitických hornin domažlické oblasti. *Sborník geologických věd, geologie* **37**, 9–70. (In Czech with English summary.)

Vejnar, Z. (1984) Magmatismus In *Geologie Domažlicke Oblasti*, eds Z. Vejnar, J. Doležal, M. Hazdrová, J. Kříž, F. Mrňa, L. Pokorný, J. Rudolsý, L. Šefrna, R. Tásler, M. Tomášek and V. Volšan, pp. 48–83. Prague (Ustøedni Ustav Geologický).

Voll, G. (1976) Recrystallization of quartz, biotite, feldspars from Erstfeld to the Leventina Nappe, Swiss Alps, and its geological significance. *Schweiz. mineral. petrogr. Mitt.* **56**, 641–647.

Watson, E. B. and Harrison, T. M. (1983) Zircon saturation revisited: temperature and composition effects in a variety of crustal magma types. *Earth and Planetary Science Letters* **64**, 295–304.

Wolf, M. B. and Saleeby, J. B. (1992) Jurassic Cordilleran dike swarm-shear zones: Implications for the Nevadan orogeny and North American plate motion. *Geology* **20**, 745–748.

Zulauf, G. (1994) Ductile normal faulting along the West Bohemian Shear Zone (Moldanubian/Teplá-Barrandian boundary) Evidence for late Variscan extensional collapse in the Variscan internides. *Geologische Rundschau* **83**, 276–292.

Zulauf, G. (1995) Cadomian and Variscan tectono–thermal events in the SW part of the Teplá-Barrandian Unit (Bohemian Massif, Czech Republic). *Zentralblatt für Geologie und Paläontologie Teil I* **1993 (9/10)**, 1515–1528.

Zulauf, G., Dörr, W., Fiala, J. and Vejnar, Z. (1997) Late Cadomian crustal tilting and Cambrian transtension in the Teplá-Barrandian unit (Bohemian Massif, Central European Variscides). Submitted to *Geologische Rundschau*.

Zulauf, G., Dörr, W. and Vejnar, Z. (1996) Thermische Modellierung des Stod-Plutons und seiner Kontaktaureole, Teplá-Barrandium. *Terra nostra* **96/2**, 209–211.